

# Shell-model phenomenology of low-momentum interactions

Achim Schwenk<sup>1,\*</sup> and Andrés P. Zuker<sup>2,†</sup>

<sup>1</sup>*Nuclear Theory Center, Indiana University, 2401 Milo B. Sampson Ln, Bloomington, IN 47408*  
<sup>2</sup>*Institut de Recherches Subatomiques, IN2P3-CNRS, Université Louis Pasteur, F-67037 Strasbourg*

The first detailed comparison of the low-momentum interaction  $V_{\text{low } k}$  with  $G$  matrices is presented. We use overlaps to measure quantitatively the similarity of shell-model matrix elements for different cutoffs and oscillator frequencies. Over a wide range, all sets of  $V_{\text{low } k}$  matrix elements can be approximately obtained from a universal set by a simple scaling. In an oscillator mean-field approach,  $V_{\text{low } k}$  reproduces satisfactorily many features of the single-particle and single-hole spectra on closed-shell nuclei, in particular through remarkably good splittings between spin-orbit partners on top of harmonic oscillator closures. The main deficiencies of pure two-nucleon interactions are associated with binding energies and with the failure to ensure magicity for the extruder-intruder closures. Here, calculations including three-nucleon interactions are most needed.  $V_{\text{low } k}$  makes it possible to define directly a meaningful unperturbed monopole Hamiltonian, for which the inclusion of three-nucleon forces is tractable.

PACS numbers: 21.60.Cs, 21.30.+x, 21.10.-k

Microscopic nuclear structure studies fall in three categories. For local interactions, the Green's Function Monte Carlo (GFMC) method [1, 2] leads to exact solutions of the many-body Schrödinger equation by evaluation of multi-dimensional integrals in coordinate space. The No-Core Shell-Model (NCSM) [3, 4] relies on matrix diagonalizations in a harmonic oscillator basis of  $N\hbar\omega$  excitations with respect to a minimal  $0\hbar\omega$  space. Convergence with  $N\hbar\omega$  is slow for conventional nucleon-nucleon (NN) potentials, which are replaced by effective interactions that are model-space dependent. Both GFMC and converged NCSM methods are limited at present to mass number  $A \lesssim 12$ . The standard Shell-Model (SM) [5] restricts diagonalizations to  $0\hbar\omega$  spaces and treats higher excitations in perturbation theory. It bypasses saturation problems by using a  $G$  matrix [6] calculated at approximately the experimental nuclear radius ( $\hbar\omega \approx 40A^{-1/3}$ ) and uses experimental single-particle energies. Presently, exact SM diagonalizations are possible for all semi-magic nuclei, and for  $A < 70$  in full  $0\hbar\omega$  spaces.

When only NN interactions are used, all microscopic approaches have a common problem, related to poor saturation and shell formation properties. It reflects in a deteriorating agreement with experiment as the number of particles increases (active particles for the  $0\hbar\omega$  SM). This leads to the conclusion that three-nucleon (3N) interactions are necessary. To constrain 3N forces, direct few-body data and some theoretical guidances are available. But restricting the studies to few-nucleon systems may not yield enough information to treat heavier nuclei.

Conventional NN interactions are well-constrained by two-nucleon scattering data only for laboratory energies  $E_{\text{lab}} \lesssim 350$  MeV. As a consequence, details of nuclear forces are not resolved for relative momenta  $k > 2.0 \text{ fm}^{-1}$ . Starting from a NN potential, the high-momentum modes can be integrated out in free space using the renormalization group. The resulting low-

momentum interaction, called  $V_{\text{low } k}$ , only has momentum components below a cutoff  $\Lambda$  and evolves with it so that all low-energy two-body observables (phase shifts and deuteron binding energy) are invariant. For  $\Lambda \lesssim 2.0 \text{ fm}^{-1}$ , all NN potentials that fit the scattering data and include the same long-distance pion physics collapse to a “universal”  $V_{\text{low } k}$  [7]. As  $V_{\text{low } k}$  does not have a strong core it can be directly used in nuclear structure calculations. This leads to a change in SM strategy that is both profound and subtle. It is profound, in that the limitations forced on the SM by hard potentials and their  $G$  matrix treatment disappear: The mean-field produced by  $V_{\text{low } k}$  will be shown to be a valuable first approximation that will greatly simplify further perturbative or coupled cluster treatment, and the inclusion of 3N forces. In particular, chiral 3N forces adjusted to  $V_{\text{low } k}$  give perturbative contributions for  $\Lambda \lesssim 2.0 \text{ fm}^{-1}$  [8] and lead to saturation in nuclear matter [9]. The subtle change follows from the close similarity that will be shown to exist between  $V_{\text{low } k}$  and  $G$  matrices. Hence the former will reproduce the successes of the latter, without the drawbacks due to the ill-defined starting energies  $\omega_s$ .

In the first part of this Letter, we compare  $V_{\text{low } k}$  with  $G$  matrices. By studying the cutoff and oscillator frequency dependence of  $V_{\text{low } k}$  matrix elements, we demonstrate a universal behavior. A similar behavior exists for  $G$  over a reasonable range of starting energies. The second part of the Letter is devoted to extracting the  $V_{\text{low } k}$  monopole Hamiltonian, which is then used to calculate binding energies, as well as single-particle and single-hole spectra on closed-shell nuclei ( $cs \pm 1$  spectra). Many features will turn out to be in good agreement with data, and the discrepancies identify what is expected of 3N forces and how they are crucial in heavier systems.

In Fig. 1, we compare  $V_{\text{low } k}$  to  $G$  matrix elements in 4 major shells. We find that both  $T = 0$  and  $T = 1$  matrix elements are very similar. For a quantitative comparison,

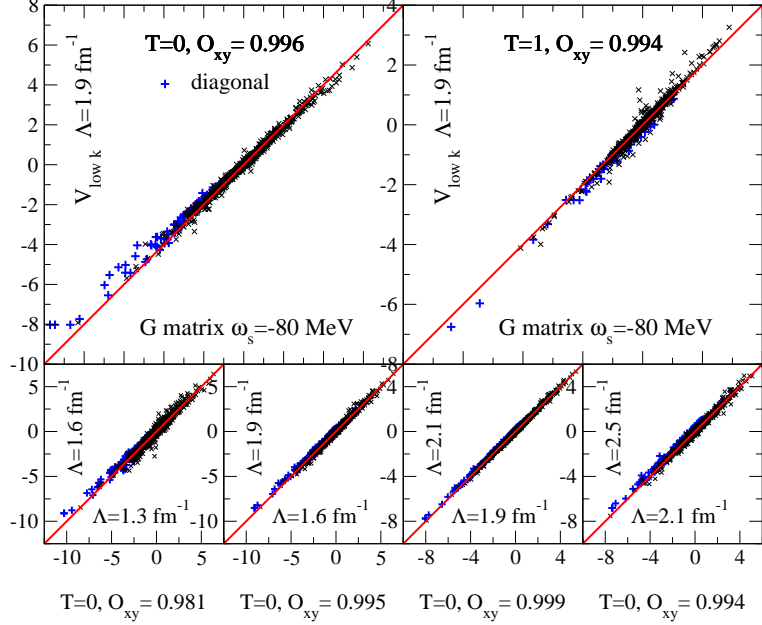


FIG. 1: (Color online) Top: Correlation plots between  $V_{\text{low } k}$  and  $G$  matrix elements in 4 major shells. The matrix elements  $V_{rstu}^{JT}$  are in MeV for  $\hbar\omega = 14$  MeV and we have highlighted the diagonal elements.  $V_{\text{low } k}$  is derived from the Argonne  $v_{18}$  potential and the  $G$  matrix is for Idaho A, computed with a rectangular Pauli operator for 4 major shells and starting energy  $\omega_s = -80$  MeV [10]. Note that for  $\Lambda = 1.9 \text{ fm}^{-1}$  the different  $V_{\text{NN}}$  have practically collapsed to one “universal”  $V_{\text{low } k}$ . Bottom: Correlation plots between  $V_{\text{low } k}$  matrix elements for different cutoffs. To facilitate the comparison, we have rescaled the  $y$ -axis set of  $V_{\text{low } k}$  matrix elements by  $\sigma_{\Lambda_x}/\sigma_{\Lambda_y}$  according to the approximate scaling law Eq. (3). The  $\sigma$ -ratios are from left to right: 1.003, 1.061, 1.050 and 1.111. We find even fewer scatters for the  $T = 1$  matrix elements. All  $O_{AB}$  given are  $O_{AB}^T$ .

we define the overlaps of interactions  $A$  and  $B$  [5, 11]

$$\sigma_{AB}^2 = d_2^{-1} \sum_{rstu\Gamma} [\Gamma] W_{rstuA}^{\Gamma} W_{rstuB}^{\Gamma}, \quad (1)$$

where  $W_{rstu}^{JT} = V_{rstu}^{JT} - \delta_{rt} \delta_{su} W$  and  $d_2$  is the dimensionality of the two-particle space, each state being counted  $[\Gamma] = (2J+1)(2T+1)$  times. Here, the interaction  $V$  is referred to its centroid  $W$ , defined by  $\sum_{rs\Gamma} [\Gamma] W_{rsrs}^{\Gamma} = 0$ . We also introduce normalized overlaps

$$O_{AB} = \frac{\sigma_{AB}^2}{\sigma_A \sigma_B}, \quad (2)$$

with  $\sigma_A = \sigma_{AA}$  and similarly  $O_{AB}^T$  for matrix elements with the same  $T$ . Interactions that differ at most by a factor  $\sigma_A/\sigma_B$  have  $O_{AB} = 1$ . The overlaps between  $V_{\text{low } k}$  and the  $G$  matrix are  $O_{AB} > 0.99$ . We have checked that a similar correlation holds between  $V_{\text{low } k}$  and  $G$  matrices computed from the Bonn potential for different model spaces with starting energies  $\omega_s = -5 \dots -140$  MeV [12].

Next, we compare  $V_{\text{low } k}$  matrix elements for different cutoffs. Over the studied range  $\Lambda = 1.3 \dots 3.0 \text{ fm}^{-1}$ , we find again very large overlaps, as shown in the bottom panels of Fig. 1. To facilitate the comparison, we have rescaled the  $y$ -axis set of  $V_{\text{low } k}$  matrix elements by the widths  $\sigma_{\Lambda_x}/\sigma_{\Lambda_y}$ . Up to this overall factor, we find that  $V_{\text{low } k}$  matrix elements are approximately cutoff-independent. From Table I, we find a similar behavior for

| $W$           | -1.374 | -1.035 | -0.802 | -0.620 | -0.546 | -0.463 |
|---------------|--------|--------|--------|--------|--------|--------|
| $\sigma_A$    | 3.288  | 2.488  | 1.931  | 1.500  | 1.323  | 1.127  |
| $\hbar\omega$ | 18.4   | 13.9   | 11.0   | 8.8    | 7.9    | 6.9    |
| 18.4          | 1.000  | 0.992  | 0.978  | 0.961  | 0.952  | 0.941  |
| 13.9          | 0.992  | 1.000  | 0.996  | 0.987  | 0.982  | 0.975  |
| 11.0          | 0.978  | 0.996  | 1.000  | 0.997  | 0.995  | 0.990  |
| 8.8           | 0.961  | 0.987  | 0.997  | 1.000  | 0.999  | 0.998  |
| 7.9           | 0.952  | 0.982  | 0.995  | 0.999  | 1.000  | 0.999  |
| 6.9           | 0.941  | 0.975  | 0.990  | 0.998  | 0.999  | 1.000  |

TABLE I: Centroids  $W$ , widths  $\sigma_A$  and overlaps  $O_{AB}$  between  $V_{\text{low } k}$  matrix elements in 4 major shells for different  $\hbar\omega$ .  $V_{\text{low } k}$  is derived from the Argonne  $v_{18}$  potential for  $\Lambda = 1.9 \text{ fm}^{-1}$ . The values of  $\hbar\omega$  correspond approximately from left to right to the double-magic nuclei at  $A = 4, 16, 40, 90, 132$  and 208.

sets with different  $\hbar\omega$  at fixed cutoff. These observations can be combined in an approximate scaling law

$$V_{\text{low } k}^{\Lambda_1, \hbar\omega_1} \approx \frac{\sigma_{\Lambda_1, \hbar\omega_1}}{\sigma_{\Lambda_2, \hbar\omega_2}} V_{\text{low } k}^{\Lambda_2, \hbar\omega_2} \Rightarrow V_{\text{low } k}^{\Lambda, \hbar\omega} \approx \sigma_{\Lambda, \hbar\omega} U, \quad (3)$$

where  $U_{rstu}^{JT}$  is a set of two-body matrix elements, approximately independent of  $\Lambda$  and  $\hbar\omega$ . Eq. (3) holds for both  $T = 0$  and  $T = 1$  matrix elements, but ratios of  $\sigma$  for the two channels are very close, so there is effectively just a

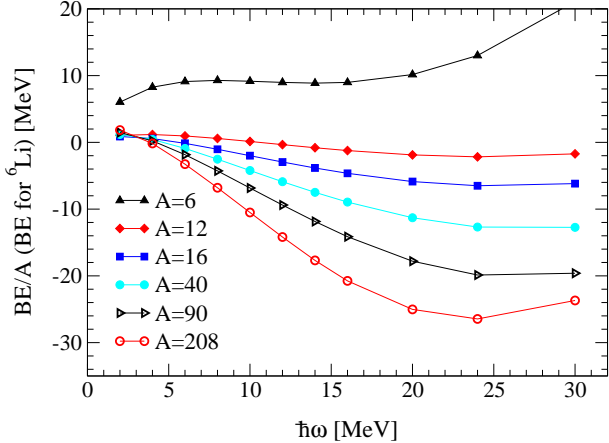


FIG. 2: (Color online) Results for the binding energies obtained from Eq. (5) (Coulomb included schematically) by filling lowest oscillator orbits.

single scaling factor. Over a wide range,  $\sigma_{\Lambda, \hbar\omega}$  scales as

$$\frac{\sigma_{\Lambda, \hbar\omega_1}}{\sigma_{\Lambda, \hbar\omega_2}} \approx \frac{\hbar\omega_1}{\hbar\omega_2} \quad \frac{\sigma_{\Lambda_1, \hbar\omega}}{\sigma_{\Lambda_2, \hbar\omega}} \approx \sqrt{\frac{\Lambda_2}{\Lambda_1}}. \quad (4)$$

These simple relationships may serve as a preliminary guide in many-body calculations. Unless otherwise noted, all following results are for the  $V_{\text{low } k}$  derived from the Argonne  $v_{18}$  potential for  $\Lambda = 1.9 \text{ fm}^{-1}$ . We have checked that, for small cutoffs, the results are practically independent of the precision nuclear force used for  $V_{\text{low } k}$ .

Next, we study binding energies of closed shell nuclei and  $cs \pm 1$  spectra. As a first approximation these are single determinantal states that do not involve configuration mixing and are described by the monopole Hamiltonian  $H_m$ . In the oscillator basis,  $H_m$  contains a diagonal and a non-diagonal part. The latter is needed for a Hartree-Fock calculation and produces further correlations [5] that will be neglected here. In neutron-proton formalism, the diagonal monopole Hamiltonian has a kinetic and a potential part,  $H_m^d = K^d + V_m^d$ , with

$$H_m^d = K^d + \frac{1}{2} \sum_{r_x, s_y} V_{r_x s_y} m_{r_x} (m_{s_y} - \delta_{r_x s_y} \delta_{xy}), \quad (5)$$

where  $x, y = n$  or  $p$ , and  $m_{r_x}$  is the number of particles in orbit  $r$  for fluid  $x$ . The centroids  $V_{r_x s_x}$  are defined in [5].

In Fig. 2, we show results for the binding energies of closed shell nuclei. In agreement with Eq. (4), we observe a linear dependence on  $\hbar\omega$  over the range in which the saturation minimum should occur once correlations and 3N forces are included. The binding energies are cutoff dependent without 3N forces. For example, in  $^{40}\text{Ca}$  at  $\hbar\omega = 12 \text{ MeV}$ , we have  $BE/A = 8.24, 5.89$  and  $4.52 \text{ MeV}$  for  $\Lambda = 1.6, 1.9$  (Fig. 2) and  $2.1 \text{ fm}^{-1}$  respectively. The case of  $^6\text{Li}$  suggests a special behavior in the light nuclei. A minimum is achieved at a reasonable  $\hbar\omega = 14 \text{ MeV}$ , although the total energy is still positive

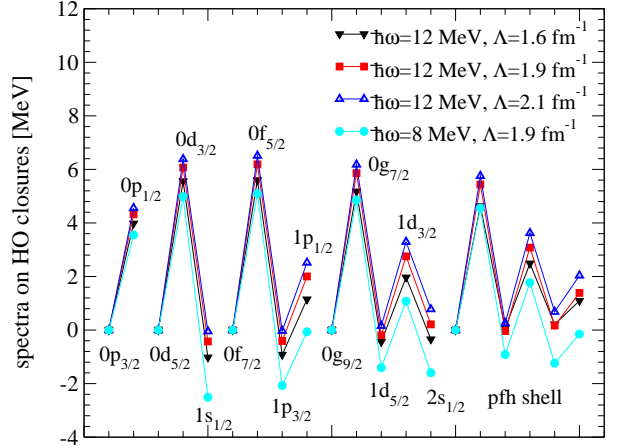


FIG. 3: (Color online) Single-particle spectra on harmonic oscillator closures. Lines (meant to guide the eye) join points belonging to the same major shell. All energies are measured from the largest  $j$  subshell in each major shell. We have used Eq. (4) to refer all  $V_{\text{low } k}$  matrix elements to  $\Lambda = 1.9 \text{ fm}^{-1}$  and rescaled by  $(\hbar\omega/\hbar\omega_0)^2 = ((p+2)^2[(p_0+2)^3+3]/(p_0+2)^2[(p+2)^3+3]^2)^2$  (see text), which corresponds to the mass number  $A$  appropriate to each major shell with principal quantum number  $p+1$ .  $p_0 = 2$  (4) correspond to the  $pf$  ( $pfh$ ) shell and  $\hbar\omega_0 = 12$  (8) MeV.

due to the competition of kinetic and potential energies  $\langle K^d \rangle = 88.0 \text{ MeV}$  and  $\langle V_m^d \rangle = -81.3 \text{ MeV}$ . This implies that configuration mixing and 3N contributions should lead to an additional 40 MeV on top of  $\langle V_m^d \rangle$ , a very reasonable expectation [4, 13].

To obtain further insight, we show the single-particle spectra on top of harmonic oscillator closures in Fig. 3. The splittings between spin-orbit partners agree well with experiment, e.g., 5.1 MeV for the  $d$  orbits in  $^{17}\text{O}$  and 6.0 MeV for the  $f$  orbits in  $^{41}\text{Ca}$ . The  $sdg$  and  $pfh$  spectra are not directly available, but they correspond nicely to those of a well-determined empirical one-body  $1 \cdot s$  force [14], that yields e.g., the same 4.6 MeV splitting for the  $h$  orbits as in Fig. 3 for  $\hbar\omega = 8 \text{ MeV}$ ,  $\Lambda = 1.9 \text{ fm}^{-1}$ . Three remarks on the  $(\hbar\omega)^2$  scaling: i) It uses  $\hbar\omega = 35.59 A^{1/3}/\langle r^2 \rangle \text{ MeV}$ , with experimental mean-square radius  $\langle r^2 \rangle = 0.943 A^{2/3} (1 + 2/A) \text{ fm}^2$  [15] and  $A \approx 2(p+2)^3/3$ , where  $p$  is the principal oscillator number at the Fermi level; ii) It complies with the physical imperative that splittings should go asymptotically as  $A^{-1/3}$ ; iii) It is not inconsistent with Eq. (4), because the matrix elements involved contribute little to  $\sigma$ .

Splittings for hole states on harmonic oscillator closures are known in  $^{15}\text{O}$  and  $^{39}\text{Ca}$  ( $\approx 6 \text{ MeV}$  in both). For  $^{15}\text{O}$  we obtain about half the observed value, in agreement with [16]. For  $^{39}\text{Ca}$  we are close at 5 MeV, as can be seen in the bottom-left panel of Fig. 4, which compares the  $cs \pm 1$  spectra in the  $pf$  shell with available data. As explained in the phenomenological study of [14], this region exhibits all the basic mechanisms of shell forma-

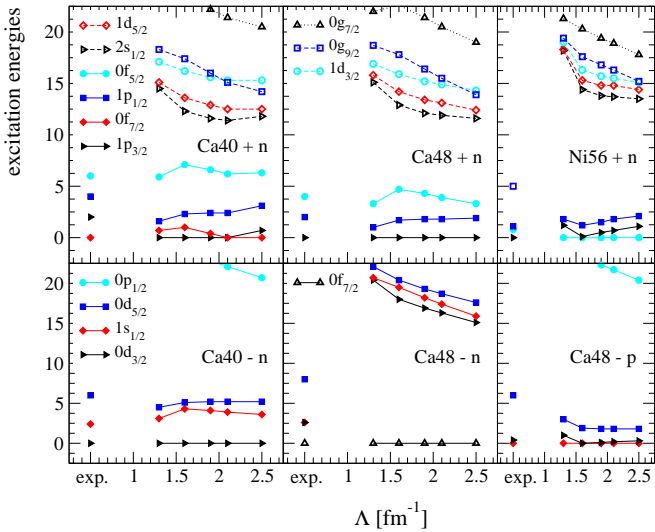


FIG. 4: (Color online)  $cs \pm 1$  spectra in the  $pf$  region for a wide cutoff range. The experimental  $0g_{9/2}$  energy in  $^{57}\text{Ni}$  is an estimate.

tion. To complete the survey of  $1 \cdot s$  properties, we note that for the uppermost levels in Fig. 4, the  $sdg$  shell, the splittings between spin-orbit partners agree with the empirical values, but smaller- $l$  orbits come too low with respect to larger- $l$  ones, accentuating a trend already apparent in Figs. 3, and partly responsible for the  $\sim 10$  MeV underbinding of the  $0g_{9/2}$  particle orbit in  $^{57}\text{Ni}$ .

The results for low-lying  $pf$  levels in the upper panel of Fig. 4 are approximately cutoff-independent and the minor discrepancies are cured by SM calculations, which push up the  $1p_{3/2}$  orbit in  $^{41}\text{Ca}$ , do not change the good spectrum in  $^{49}\text{Ca}$ , and also push up by 1 MeV the  $0f_{5/2}$  orbit in  $^{57}\text{Ni}$  [5, 17]. For the hole states in the lower panel, we find that the  $0f_{7/2}$  orbit in  $^{47}\text{Ca}$  is underbound by  $\sim 10$  MeV, a phenomenon associated to the failure of NN forces to ensure the  $N, Z = 28, 50, 82 \dots$  extruder-intruder magicity [5, 18]. This can be directly checked through the standard measures of magicity, the gaps defined as  $g(cs, x) = 2BE(cs) - BE(cs + x) - BE(cs - x)$  ( $x = n$  or  $p$ ). Rounded calculated (experimental) gaps are (in MeV):  $g(^{40}\text{Ca}, n) = 13(7)$ ,  $g(^{48}\text{Ca}, p) = 17(6)$ ,  $g(^{48}\text{Ca}, n) = -0.4(5)$  and  $g(^{56}\text{Ni}, n) = 0.5(6)$ . Hence, we find that extruder-intruder closures are non-existent, and harmonic oscillator closures are too strong. A related problem is that the  $0d_{5/2}$  hole orbits in  $^{47}\text{Ca}$  and  $^{57}\text{Ni}$  are underbound by  $\sim 4$  MeV with respect to their  $sd$  counterparts. On the contrary the  $1s_{1/2} - 0d_{3/2}$  splittings are quite good: Although too large by some 1.5 MeV in  $^{39}\text{Ca}$ , in  $^{47}\text{Ca}$  the splitting is drastically reduced, close to what the data demand, and further reduced in  $^{47}\text{K}$ , now very close to experiment.

Thus, we find that when the largest orbit in a major shell fills, it binds itself and contributes to the binding of the largest orbits in neighboring shells in a way that

NN forces fail to reproduce. The intra-shell self-binding is now well understood in terms of a 3N mechanism [19]. In this Letter we have identified the precise nature of the cross-shell binding problem. A revision of the phenomenology of [14] in terms of 3N forces is called for and may be of help in a more fundamental approach.

In summary, we have shown that  $V_{\text{low } k}$  and  $G$  matrix elements are quantitatively similar, but  $V_{\text{low } k}$  as a free-space potential is far easier to use in many-body calculations. It leads to matrix elements that are approximately cutoff and oscillator frequency independent up to an overall scaling with the width of the interaction. In a pure NN description,  $V_{\text{low } k}$  reproduces many features of the  $cs \pm 1$  spectra, and makes it clear that, apart from saturation, the main problem that demands a 3N treatment is related to extruder-intruder shell formation.

We thank Hans Feldmeier and Dick Furnstahl for useful discussions. The work of AS is supported by the DOE Grant No. DEFG 0287ER40365 and NSF Grant No. nsf-phy 0244822.

\* E-mail: schwenk@indiana.edu

† E-mail: Andres.Zuker@IReS.in2p3.fr

- [1] S. C. Pieper and R. B. Wiringa, Ann. Rev. Nucl. Part. Sci. **51**, 53 (2001).
- [2] S. C. Pieper, R. B. Wiringa, and J. Carlson, Phys. Rev. C **70**, 054325 (2004).
- [3] P. Navrátil, J. P. Vary, and B. R. Barrett, Phys. Rev. C **62**, 054311 (2000).
- [4] P. Navrátil and E. Caurier, Phys. Rev. C **69**, 014311 (2004).
- [5] E. Caurier, G. Martínez-Pinedo, F. Nowacki, A. Poves, and A. P. Zuker, nucl-th/0402046, to appear in Rev. Mod. Phys.
- [6] M. Hjorth-Jensen, T. T. S. Kuo, and E. Osnes, Phys. Rept. **261**, 126 (1995).
- [7] S. K. Bogner, T. T. S. Kuo, and A. Schwenk, Phys. Rept. **386**, 1 (2003), for RG details see nucl-th/0111042.
- [8] A. Nogga, S. K. Bogner, and A. Schwenk, Phys. Rev. C **70**, 061002(R) (2004).
- [9] S. K. Bogner, A. Schwenk, R. J. Furnstahl, and A. Nogga, in preparation.
- [10] D. J. Dean and M. Hjorth-Jensen, private communication.
- [11] M. Dufour and A. P. Zuker, Phys. Rev. C **54**, 1641 (1996).
- [12] M. Hjorth-Jensen, private communication.
- [13] L. Coraggio, N. Itaco, A. Covello, A. Gargano, and T. T. S. Kuo, Phys. Rev. C **68**, 034320 (2003).
- [14] J. Duflo and A. P. Zuker, Phys. Rev. C **59**, R2347 (1999).
- [15] J. Duflo and A. P. Zuker, Phys. Rev. C **66**, 051303(R) (2002).
- [16] S. C. Pieper and V. R. Pandharipande, Phys. Rev. Lett. **70**, 2541 (1993).
- [17] F. Nowacki, private communication.
- [18] E. Pasquini and A. P. Zuker, in *Physics of Medium Light Nuclei, Florence 1977*, edited by P. Blasi (Editrice Compositrice, Bologna, 1978).
- [19] A. P. Zuker, Phys. Rev. Lett. **90**, 042502 (2003).